Modelling and Simulation Testing of Main Bearing Loads and Strains in Crankshafts Caused by Deviations in the Position of the Shaft Journal and Bearing Axes

sciendo

doi:10.2478/mape-2020-0004

Date of submission to the Editor: 03/2020
Date of acceptance by the Editor: 06/2020

MAPE 2020, volume 3, issue 1, pp. 41-56

Krzysztof Nozdrzykowski
ORCID ID: 0000-0003-2785-0868

Zenon Grządziel
ORCID ID: 0000-0001-9348-1111
Maritime University of Szczecin, **Poland**

INTRODUCTION

Crankshafts of a ship's main propulsion power machines as well as auxiliary engines are one of the most important elements of the crank-piston system, and perform rotary movement supported by bearings in the engine block. Sliding bearings are commonly used in this type of design, currently, most often fitted with the so called flexible multilayer thin-walled bushings. The use of this type of bearings is dictated by a number of proven and unquestionable advantages of thin-walled bushings over traditional solutions such as rigid thick-walled bushings. To some extent, they maintain their shape and dimensions, regardless of the housing in which they are mounted. Exclusive use of flexible bushings in railway and marine engines is characterized by the fact that their flexible design is unable to provide the appropriate rigidity and geometric shape of the bearing, and hence, these functions are facilitated by the bearing socket. The thickness of the flexible bushings must be within close tolerances to ensure the required clearance value in relation to the journal and the exact circumferential length, which results in its compression into the socket. This pressure should guarantee the appropriate values of radial surface pressures and, as a result the friction forces at the contact between the bushings and the socket should ensure its rotation in the socket. Regardless of the design of the bushings, the most important dimension determining the correct functioning of the crank-piston system for shaft bearing is the bearing clearance (Łukomski, 1972; Kozłowiecki, 1974; Basiński and Szyndler, 1984; Barwell, 1984).

In most of the available studies concerning the analysis of factors influencing the change in the practical value of bearing clearance, the impact of geometrical deviations of the bearing system (especially crankshafts) is marginalized. The measuring techniques currently in use lack the equipment and instruments to accurately assess the geometric condition of crankshafts. Therefore, such measurements are usually carried out with the use of conventional measuring

Contact address: z.grzadziel@am.szczecin.pl

equipment, the accuracy of which is not adjustable in accordance with the manufactured shafts.

The measurement system enabling a correct and comprehensive assessment of the geometric condition of large-size crankshafts has been developed in the Cathedral of Basic Engineering and Materials Science of the Maritime University of Szczecin. This system is equipped with a flexible support system for the measured object, compensating the elastic deformations of the shaft due to its own weight; whereby the measurements of large-size crankshafts can be carried out in conditions corresponding to the non-reference measurements when determining the object measured in counterpoints (Nozdrzykowski, 2013; Nozdrzykowski, 2017; Nozdrzykowski, 2015; Nozdrzykowski, 2011a; Nozdrzykowski, 2011b).

Fig. 1 shows a constructed test rig operating according to the adopted concept of the measuring system, equipped with a flexible support system for the measured object.

Fig. 1 The prototype test rig developed at the Maritime University of Szczecin for measuring geometrical deviations of large crankshafts with a flexible support system

Source: prepared by the authors

The authors have conducted a number of studies justifying the purposefulness and necessity to measure both the shape and positional deviations of the crankshaft journals axes, for which the proposed measurement system has proved to be entirely relevant. The research results are presented subsequently.

MATCHING THE BEARING CLEARANCE – EXAMPLES OF CALCULATIONS

Plain bearing clearance, as previously highlighted, is one of the most important factors determining its operation, especially in the case of hydrodynamic lubrication. The clearance distribution depends on the difference between journal and socket diameters and deviations in shape. Numerous experimental and theoretical works have shown that a change in bearing clearance causes a change in all parameters for bearing operation. Given the complexity of the issue

and the challenge of taking into account all the factors influencing the thickness of the lubricant layer under actual operating conditions, the theoretical evaluation of the optimum clearance is not always precise. It is important to take into account the presumed bearing load capacity, the minimum thickness of the lubricant layer, the lubricant flow and operating temperature as well as the journal and bushings sliding layer materials when analyzing the clearance matching. The theoretical basis for this was developed by Gläser and Gnilke (Kozłowiecki, 1974). A more precise selection of bearing clearance values allows to obtain various empirical or semi-empirical formulas, tables and diagrams related to the state during bearing operation (operating clearance) or to the conditions during assembly (mounting clearance). The knowledge of the working clearance is essential for calculating the plain bearing. Moreover, knowledge of the mounting clearance together with appropriate tolerances is essential for the correct manufacturing and assembly of a bearing. A pragmatic formula for optimal matching of bearing clearance for sliding bearings of fast and medium-speed internal combustion engines, according to Glacier Co United Kingdom (Kozłowiecki, 1974):

$$L_{m\,opt} = \frac{n^{0.5} d^{2,5}}{46 \cdot 10^3} \tag{1}$$

For the other types of motors, the clearance should be determined according to the formula:

$$L_{m\,opt} = \frac{n^{0.25}\, d}{6} \tag{2}$$

where:

L_m – optimal mounting clearance in diameter [mm],

d – nominal journal diameter [mm],

n – rotational speed [rpm].

Kingsbury (Kozłowiecki, 1974), gives a less complex relation which allows the selection of bearing clearance in diameter, depending solely on the journal diameter:

$$L_m = 0.005 + 0.001 \cdot d \tag{3}$$

Recommended clearance values are quite often expressed in relative form (most often in relation to the journal diameter). Such form is preferred by Vogelpoll (Kozłowiecki, 1974), making the selection of the working value of relative bearing clearance dependent on the journal circumferential speed. It is expressed as a function:

$$\psi = 0.8 \cdot 10^{-3} \cdot \sqrt[4]{v}\,(1 \pm 0.3) \tag{4}$$

where:

v – journal circumferential speed [m/s].

The relative form of the recommended clearance value is also given by Willi and Kamps (Kozłowiecki, 1974).

In the case of Willi and Kamps, the relative clearance value is determined by the sliding layer material:

– for a sliding layer made of white material adopt $\psi = 0.0005$,

– for a sliding layer made of Cd-Ag-Cu alloy adopt ψ = 0.0008,
– for a sliding layer made of Cu-Pb alloy adopt ψ = 0.001.

Above are recommended relative clearance values for a specific engine group. The author states that in the case of moderate duty marine engines, the relative clearance should be between ψ = 0.5÷0.8‰.

Table 1 shows examples of clearance values evaluated on the basis of prepared diagrams facilitating the mounting clearance matching for the main bearings of the crankshaft of the medium-rotational engine of the Buckau Wolf R8 DV136 main propulsion vessel.

Table 1 Example of clearance value calculations carried out for the main crankshaft bearings of a ship's medium-rotation main propulsion Buckau Wolf R8 DV136 engine

Source/ relation no.	Relation	Recommended absolute (L_m) or relative (ψ_m) mounting clearance in diameter	Notes
Glacier Co. G.B. (Kozłowiecki, 1974; Basiński and Szyndler, 1984)/(1)	$L_{m\,opt} = \frac{n^{0.5} d^{2,5}}{46 \cdot 10^3}$	$L_{m\,opt}$ = 0.1136 mm	Where: d = 150 mm and n = 360 rpm
Glacier Co. G.B. (Kozłowiecki, 1974; Basiński and Szyndler, 1984)/(1)	$L_{m\,opt} = \frac{n^{0.25}\, d}{6}$	$L_{m\,opt}$ = 0.1089 mm	Where: d = 150 mm and n = 360 rpm
Kingsbury (Kozłowiecki, 1974)/(2)	L_m = 0.005+0.001 d	L_m = 0.1550 mm	Where: d = 150 mm
Vogelpoll (Kozłowiecki, 1974/(3)	$\psi = 0.8 \cdot 10^{-3}\ \sqrt[4]{v}\,(1 \pm 0.3)$	ψ = 0.0003134·(1±0.3) L_m = (0.047÷0.0611) mm	Where: v = 0.02355 m/s
Willi; Kamps (Kozłowiecki, 1974)/(4)	ψ = 0.5÷0.8‰	L_m = (0.075÷0.120) mm	
Milowiz (Kozłowiecki, 1974)/(5)	$L_{m\,min} = 0.9 \cdot \psi \cdot d \le L_m \le 1{,}3 \cdot \psi \cdot d = L_{m\,max}$	L_m = (0.045÷0.097) mm	Where: ψ = 0.5‰ and d = 150mm
		L_m = (0.108÷0.157) mm	Where: ψ = 0.8‰ and d = 150mm
Glacier – Metal Co. (Kozłowiecki, 1974; Basiński and Szyndler, 1984)	Graph	L ≈ 0.09 mm	Where: d = 150mm and n=360 rpm
Glyco – Metal Wiesbaden (Kozłowiecki, 1974; Basiński and Szyndler, 1984)	Graph	L ≈ 0.11 mm	Where: d = 150 mm and n = 360 rpm

According to the presented recommendations given in the available source materials, the clearance values and the mounting clearance tolerances (boundary clearances) may vary considerably depending on the interpretation. Therefore, the proposal of Milowiza is advantageous in establishing clearance limits. It is recommended that mounting clearance should be accepted within the boundaries:

$$L_{m\,min} = 0.9 \cdot \psi \cdot d \le L_m \le 1.3 \cdot \psi \cdot d = L_{m\,max} \quad (5)$$

From a geometric point of view, the minimum "cold" clearance is determined structurally by means of an appropriate selection of the journal dimensions and dimensional deviations, the socket diameter and the thickness of the bushings, and the increase in the socket diameter caused by the compression.

INFLUENCE OF GEOMETRICAL DEVIATIONS ON THE BEARINGCLEARANCE DISTRIBUTION

The aforementioned crankshaft, for which exemplary calculations of the recommended clearance values have been made (Table 1), is the object under investigation. The aim of the research was to verify and implement an innovative measurement system with the so-called flexible support of the measured object, developed at the Maritime Academy in Szczecin. The system enables, as previously highlighted, measurements of geometric deviations of large-size crankshafts in conditions corresponding to the non-reference measurements determining the shaft measured in counterpoints.

The difference between a real bearing and an ideal bearing is defined as the interaction of two ideal cylinders that can be very large in reality where the geometry of the lubrication space of both bearings is compared. The journal, socket and bushing can have different regular or irregular shape contours in both transverse and longitudinal cross-sections. The axes of the individual shaft journals and sockets can be diagonally positioned in relation to each other as a result of machining errors, wear, and elastic or thermal deformation caused by operating conditions. Due to these errors, the actual minimum thickness of the lubricating film can often be less than the minimum calculated under the assumption of perfect shapes and concentricity. Fig. 2 illustrates the complexity of the geometry of the bearing clearance space when only the single crankshaft plain bearing is considered. One of the possible shape and axis error position of the components forming a single sliding bearing with the so-called flaccid thin-walled bushings is shown in Fig. 2 in the longitudinal and transverse cross-section.

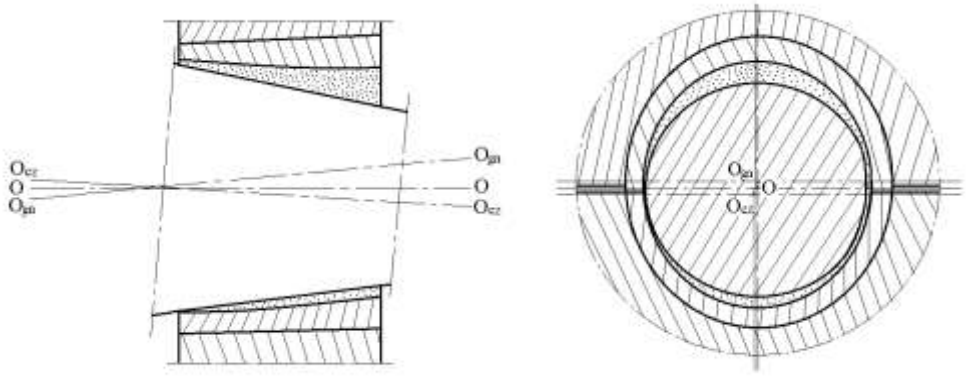

Fig. 2 Example of shape and axis overlap of the components forming a single slide bearing equipped with so-called flaccid thin-walled bushings

Based on the thin bearing theory, a correlation can be derived to determine the maximum allowable misalignment of the journal and pans mounted in the socket (Barwell, 1984).

$$\frac{P}{\eta v}\left(\frac{h_m}{b}\right)^2 = \frac{\pi}{4}\frac{\lambda}{(1+\lambda)^2}(1+0.62\lambda^2)^{1/2} \quad (6)$$

where:
P – Load (per unit of width) [N/m],
η – absolute viscosity [Pa·s],
v – tangent speed toward surface [m/s],
h_m – the thickness of the lubricating layer at the point of greatest proximity [mm],
b – bearing width in the direction perpendicular to motion [mm],
λ – relative eccentricity e/L,
e – eccentricity [mm],
L – radial clearance [mm].
Equation (6) applies when a bearing with misalignment is under investigation during operation. The practical application of this equation is illustrated in Fig. 3. In case of ideal concentricity shown in Fig. 3a:

$$h_m = L\,(1 - \lambda) \quad (7)$$

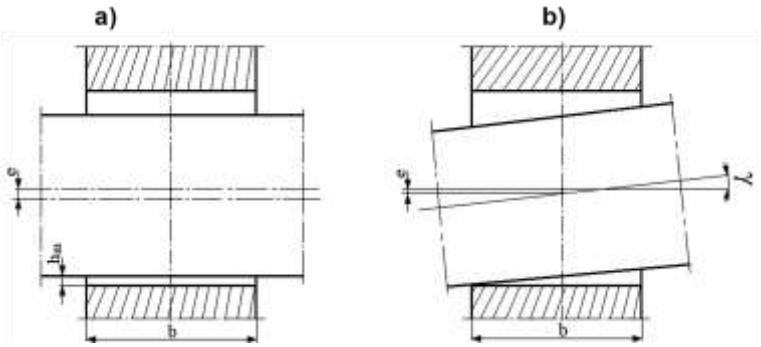

Fig. 3. a) Slide bearing with journal axles and socket arranged coaxially, b) slide bearing with journal axles and socket that are not arranged coaxially

Taking into account, the probability of coaxial misalignment, the axes of the journal and the pan hole can take the reciprocal position as in the Fig. 3b. The coaxial misalignment defined by angle γ can then be expressed by the following equation:

$$tan\,\gamma = \frac{2 \cdot L}{b}(1 - \lambda) \quad (8)$$

The dependence on the maximum value of the eccentricity at a given size disturbance angle γ can be:

$$\lambda_{max} = 1 - a \quad (9)$$

where:
the variable a = (b/2l)·tgγ is referred to as the dimensionless number of size disturbance (Barwell, 1984).
With a relative eccentricity of *λ* = 0, the bearing ability to transfer loads disappears and consequently the shaft comes into contact with the bushing at its edge. Thus, the possibility of running the transverse sliding bearings under conditions where the geometric size of the shaft journal axis and pan hole is disturbed is significantly reduced. Following equation (6) there is no benefit in

increasing clearance when λ reaches 0.78, in this case the allowable misalignment is given by the relation (Barwell, 1984):

$$tan\,\gamma \leq \left(\frac{\eta \cdot v}{P}\right)^{1/2} \cdot 0.98 \quad (10)$$

The case of eccentricity of the elements forming the sliding bearing shown in Fig. 3b describes a journal as an ideal cylinder whose axis is non-deformable. Due to the interconnection and interaction of the interlinked, individual crankshafts are deformed differently, and the journal axes also undergoes a variety of bends and torsional elastic deformations. Consequently, this leads not only to a change in clearance but also to rapid, dynamic changes in the value of reaction forces in the bearings during shaft rotation. These observations are confirmed by the results of simulation tests carried out to assess the influence of geometrical deviations of the bearing system upon the values of main bearing loads and strains in crankshafts.

MODELING AND SIMULATION RESEARCH CONCERNING THE INFLUENCE OF GEOMETRICAL DEVIATIONS OF THE BEARING SYSTEM ON THE VALUES OF MAIN BEARING LOADS AND STRAINS IN CRANKSHAFTS

Simulation tests were carried out using the Midas NFX 2019 simulation program based on FEM. The aforementioned crankshaft of the medium-rotation main Buckau Wolf R8DV 136 engine of the vessel was modeled. The crankshaft was 3630 mm long and 9280 N heavy, with ten 149 mm diameter main journals and eight 144mm diameter crank journals, Fig. 4.

Fig. 4 Modeled medium speed crankshaft of the Buckau Wolf R8DV 136 main drive

Analysis of deformations and reaction forces, with consideration of the recommended clearance value and shaft weight in relation to the assumed inaccuracies with regard to the position of journal and socket axes of individual main bearings, was made for subsequent angular shaft positions, in the range of 0°-360°, changing its position every 15°.

Simulation tests were conducted for a number of possible inaccuracies in the crankshaft bearing. Given the abundant research material, this publication is limited to a selection of the most representative cases considered:

- case no. 1: the axes of the individual main bearing sockets are perfectly coaxial, while one of the axes of the crankshaft main journals (journal axis No. 4, counting from the camshaft wheel side) is moved upwards by 0.03 mm from the others;
- case no. 2: all axes of the crankshaft journals are perfectly coaxial, while one of the axes of the main bearing sockets (socket axis No. 5, counting from the camshaft side) is shifted upwards by 0.03 mm from the others;
- case no. 3: one of the axes of the main bearing sockets (socket axis No. 6, counting from the camshaft wheel side), is moved upwards by 0.03 mm from the others, and one of the axles of the crankshaft main journals (journal axis No. 4, counting from the camshaft side) is offset from the others downwards by 0.03 mm.

The results of the tests are shown in the form of tables and diagrams representing the values of reaction forces occurring in the vertical and horizontal plane on individual main bearings and in the form of examples of strain values presented for selected angular shaft positions.

Table 2 and diagrams in Fig. 5 show (Polar and Cartesian coordinate system), values of reaction forces occurring in the vertical plane.

Table 2 Distribution of vertical reaction forces in the bearings when the individual main bearing sockets axes are perfectly coaxial, while one of the crankshaft main journals axles (journal axis No. 4, counting from the camshaft wheel side) is moved upwards by 0.03 mm from the others

	Angle [° CA]																								
Journal No.	0	15	30	45	60	75	90	105	120	135	150	165	180	195	210	225	240	255	270	285	300	315	330	345	360
1	650	648	666	701	746	792	831	856	865	860	845	826	811	804	806	815	826	833	831	814	785	746	705	671	650
2	1216	1226	1187	1105	995	875	768	689	647	643	668	707	745	772	780	773	760	754	768	811	883	976	1075	1161	1216
3	-1028	-1010	-822	-474	2	556	1132	1677	2142	2494	2720	2819	2802	2689	2495	2234	1916	1547	1132	686	227	-214	-597	-880	-1028
4	7936	7774	7110	5988	4493	2744	883	-941	-2589	-3948	-4932	-5493	-5616	-5316	-4626	-3594	-2283	-764	883	2567	4187	5635	6804	7597	7936
5	-9757	-9437	-8373	-6635	-4350	-1690	1141	3935	6491	8634	10230	11189	11463	11053	9995	8363	6257	3799	1141	-1554	-4115	-6364	-8138	-9301	-9757
6	9425	9168	8317	6934	5125	3027	802	-1386	-3382	-5054	-6298	-7046	-7263	-6951	-6135	-4866	-3219	-1292	802	2933	4962	6746	8154	9073	9425
7	-2468	-2404	-2073	-1496	-721	180	1126	2036	2839	3477	3920	4153	4180	4017	3684	3205	2603	1900	1126	316	-485	-1224	-1837	-2268	-2468
8	1738	1788	1745	1611	1402	1148	888	661	497	410	398	445	528	618	697	755	797	834	888	975	1102	1266	1446	1615	1738
9	985	941	931	959	1018	1095	1170	1226	1249	1235	1189	1124	1061	1014	996	1012	1056	1115	1170	1206	1211	1181	1123	1052	985
10	581	591	594	588	575	558	541	530	527	532	545	561	577	588	591	586	573	557	541	531	528	535	548	565	581

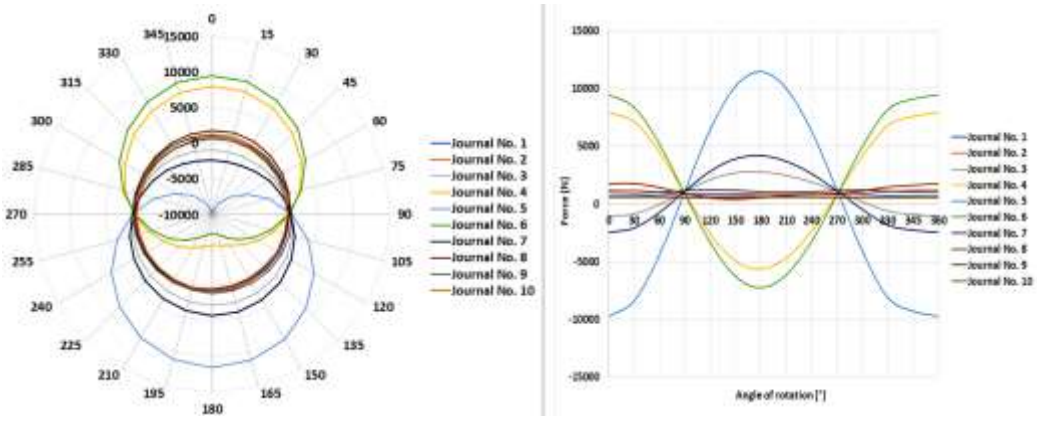

Fig. 5 Polar and Cartesian distribution diagrams of the vertical reaction forces in bearings where the individual main bearing sockets axes are perfectly coaxial, one of the crankshaft main journals axes (journal axis No. 4, counting from the camshaft side) is shifted upwards by 0.03 mm from the others

Table 3 and diagrams in Fig. 6 show the values of reaction forces occurring in the horizontal plane for the variant formulated as case no. 1.

Table 3 Distribution of horizontal reaction forces in bearings where the axles of the individual main bearing sockets are perfectly coaxial, one of the crankshaft journals axles (journal axis No. 4, counting from the camshaft side) is moved upwards by 0.03 mm from the others

	Angle [°CA]																							
Journal No.	0	15	30	45	60	75	90	105	120	135	150	165	180	195	210	225	240	255	270	285	300	315	330	345	360
1	0	49	95	129	147	145	126	95	60	30	8	-1	0	8	15	16	8	-10	-35	-61	-79	-85	-73	-43	0
2	0	-123	-242	-338	-393	-401	-365	-295	-209	-125	-58	-16	0	-1	-7	-5	15	53	106	159	199	208	177	105	0
3	1	575	1129	1607	1960	2154	2175	2030	1747	1361	916	451	-1	-419	-788	-1103	-1358	-1547	-1655	-1668	-1569	-1345	-997	-538	1
4	-8	-1853	-3600	-5108	-6253	-6944	-7129	-6805	-6012	-4827	-3353	-1702	8	1671	3190	4486	5491	6151	6423	6281	5716	4743	3409	1790	-1
5	16	2846	5503	7782	9513	10571	10881	10425	9261	7487	5239	2679	-16	-2674	-5131	-7238	-8871	-9929	-10339	-10055	-9091	-7489	-5339	-2779	16
6	-10	-2249	-4344	-6136	-7489	-8305	-8533	-8166	-7246	-5853	-4095	-2095	10	2089	4016	5678	6973	7819	8156	7949	7196	5933	4233	2205	-10
7	1	946	1848	2622	3200	3532	3596	3396	2965	2351	1612	810	-1	-776	-1479	-2081	-2559	-2890	-3052	-3024	-2791	-2349	-1710	-909	1
8	1	-240	-495	-723	-889	-968	-951	-846	-677	-478	-283	-118	0	73	110	133	159	201	260	324	372	378	323	195	1
9	0	61	138	211	263	280	260	206	135	64	10	-13	0	42	100	158	198	207	184	134	70	11	-27	-32	0
10	0	-15	-31	-47	-58	-61	-55	-42	-26	-9	2	5	0	-12	-29	-44	-55	-58	-52	-39	-22	-7	4	6	0

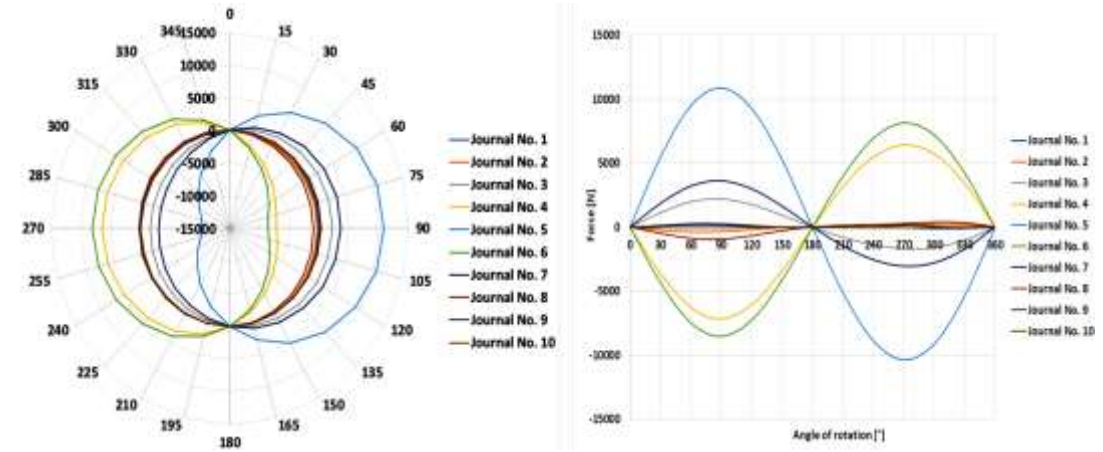

Fig. 6 Polar and Cartesian plots of the horizontal reaction forces in bearings where the axes of individual main bearing sockets are perfectly coaxial, one of the crankshaft main journal axles (journal axis No. 4, counting from the camshaft side) is moved upwards by 0.03 mm from the others

Fig. 7 shows an example of the distribution of reduced strain occurring along the length of the shaft in an angular position equal to 180°.

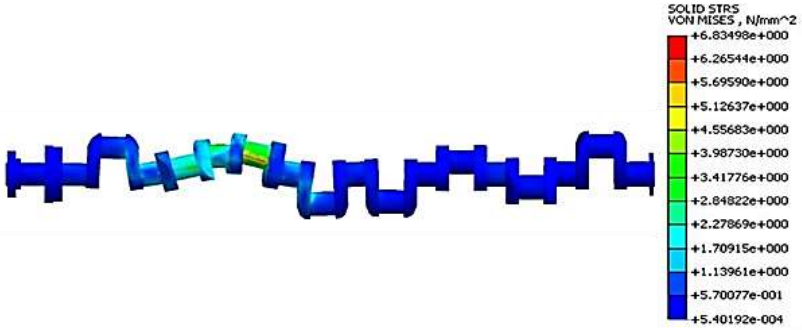

Fig. 7 Reduced stress distribution along the shaft length, when the axes of the individual main bearing sockets are perfectly coaxial, one of the crankshaft main journal axes (journal axis No. 4, counting from the camshaft side) is moved upwards by 0.03 mm from the others – angular position of the shaft equivalent to 180°

Table 4 and diagrams in Fig. 8 show (Polar and Cartesian coordinate system), the values of vertical reaction forces.

Table 4 Distribution of the reaction forces considered in the vertical plane for the case where all axes of the crankshaft main journals are perfectly coaxial, one of the main bearing socket axes (socket axis 5, counting from the camshaft side) is shifted upwards by 0.03 mm from the others

	Angle [° CA]																							
Journal No.	0	15	30	45	60	75	90	105	120	135	150	165	180	195	210	225	240	255	270	285	300	315	330	345	360
1	811	810	829	864	905	941	963	964	944	910	869	833	811	810	829	864	905	941	963	964	944	910	869	833	811
2	745	732	629	466	285	135	56	70	172	336	517	667	745	732	629	466	285	135	56	70	172	336	517	667	745
3	2802	2848	3104	3501	3934	4285	4461	4416	4160	3763	3331	2979	2802	2848	3104	3501	3934	4285	4461	4416	4160	3763	3331	2979	2802
4	-5616	-5642	-5902	-6325	-6797	-7193	-7406	-7378	-7118	-6696	-6223	-5828	-5616	-5642	-5902	-6325	-6797	-7193	-7406	-7578	-7118	-6696	-6223	-5828	-5616
5	11463	11393	11363	11383	11450	11529	11615	11685	11704	11684	11628	11549	11463	11393	11363	11383	11450	11529	11615	11685	11704	11684	11628	11549	11463
6	-7263	-7116	-6820	-6454	-6116	-5896	-5853	-5999	-6294	-6661	-6999	-7220	-7263	-7116	-6820	-6454	-6116	-5896	-5853	-5999	-6294	-6661	-6999	-7220	-7263
7	4180	4031	3760	3441	3159	2989	2977	3126	3397	3715	3998	4168	4180	4031	3760	3441	3159	2989	2977	3126	3397	3715	3998	4168	4180
8	528	627	727	799	826	799	726	626	526	454	428	454	528	627	727	799	826	799	726	626	526	454	428	454	528
9	1061	1015	1001	1023	1073	1141	1206	1252	1266	1245	1193	1126	1061	1015	1001	1023	1073	1141	1206	1252	1266	1245	1193	1126	1061
10	577	588	590	583	569	552	536	525	523	530	543	561	577	588	590	583	569	552	536	525	523	530	543	561	577

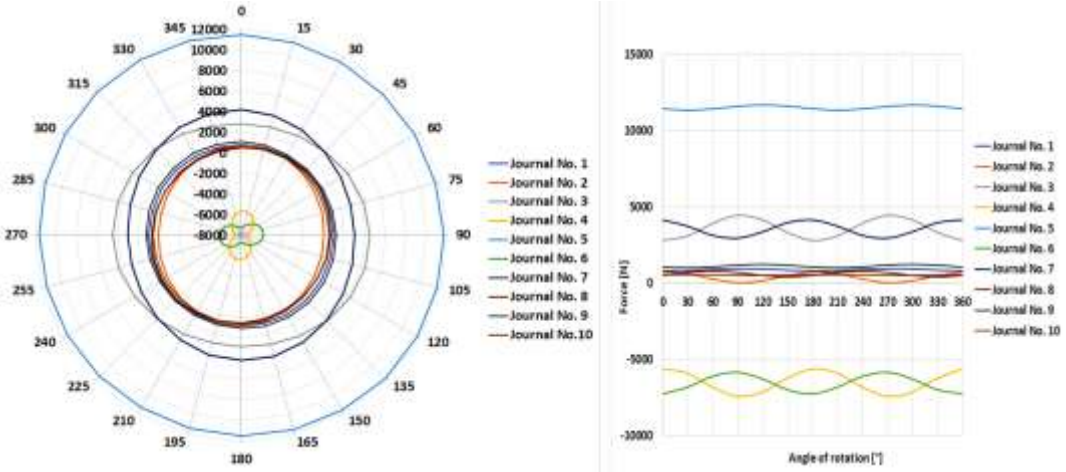

Fig. 8 Polar and Cartesian distribution diagrams of the vertical reaction forces in bearings where all axes of the crankshaft main journal axes are perfectly coaxial, one of the main bearing socket axes (socket axis No. 5, counting from the camshaft side) is shifted upwards by 0.03mm from the others

Table 5 and diagrams in Fig. 9 show the values of horizontal reaction forces for the variant formulated as case no. 2.

Table 5 Distribution of horizontal reaction forces in bearings where all crankshaft journal axes are perfectly coaxial, one of the axes of the main bearing sockets (socket axis No. 5, counting from the camshaft side) is shifted upwards by 0.03 mm from the others

	Angle [° CA]																							
Journal No.	0	15	30	45	60	75	90	105	120	135	150	165	180	195	210	225	240	255	270	285	300	315	330	345	360
1	0	41	77	99	100	80	46	5	-31	-53	-54	-35	0	41	77	99	100	80	46	5	-31	-53	-54	-35	0
2	0	-181	-331	-409	-396	-293	-130	51	201	280	266	164	0	-181	-331	-409	-396	-293	-130	51	201	280	266	164	0
3	-1	431	783	959	914	658	260	-172	-524	-700	-655	-399	-1	431	783	959	914	658	260	-172	-524	-700	-655	-399	-1
4	8	-464	-859	-1072	-1045	-785	-362	110	506	718	691	431	8	-464	-859	-1072	-1045	-785	-362	110	506	718	691	431	8
5	-16	44	128	214	280	306	287	227	143	57	-9	-35	-16	44	128	214	280	306	287	227	143	57	-9	-35	-16
6	10	348	569	611	465	169	-197	-536	-756	-799	-653	-357	10	348	569	611	465	169	-197	-536	-756	-799	-653	-357	10
7	-1	-283	-453	-465	-316	-46	273	555	725	787	588	318	-1	-283	-453	-465	-316	-46	273	555	725	787	588	318	-1
8	0	27	0	-74	-173	-273	-346	-372	-345	-272	-172	-72	0	27	0	-74	-173	-273	-346	-372	-345	-272	-172	-72	0
9	0	51	118	184	229	243	222	170	103	38	-8	-22	0	51	118	184	229	243	222	170	103	38	-8	-22	0
10	0	-14	-31	-47	-58	-60	-54	-40	-22	-6	4	7	0	-14	-31	-47	-58	-60	-54	-40	-22	-6	4	7	0

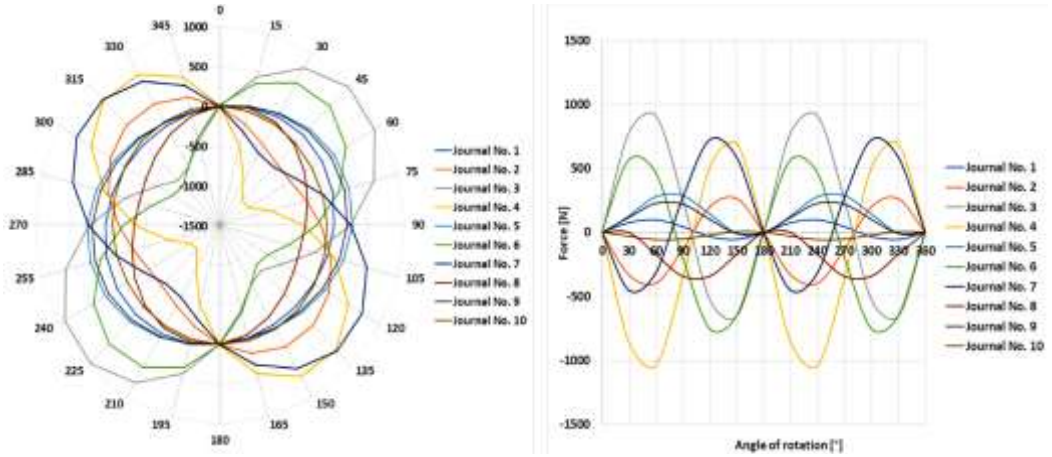

Fig. 9 Polar and Cartesian plots of the horizontal reaction forces in the bearings where all crankshaft journal axes are perfectly coaxial, one of the main bearing socket axes (socket axis No. 5, counting from the camshaft side) is shifted upwards by 0.03 mm from the others

Fig. 10 shows an example of the strain distribution along the shaft length.

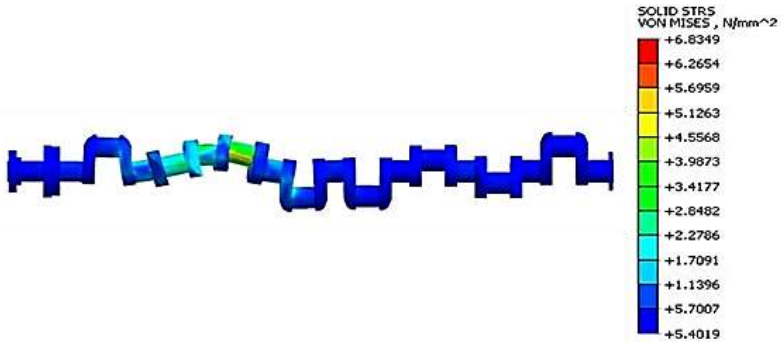

Fig. 10 Reduced stress distribution along the shaft length where all crankshaft journal axes are perfectly coaxial, one of the main bearing socket axes (socket 5 axis, counting from the camshaft wheel side) is shifted upwards by 0.03 mm from the others – angular position of the shaft equivalent to 180°

Table 6 and diagrams in Fig. 11 show (Polar and Cartesian coordinate system), the values of vertical reaction forces.

Table 6 Distribution of the vertical reaction forces for the case where one of the main bearing socket axes (socket axis No. 6, counting from the camshaft sprocket side) is shifted upwards from the others by 0.03 mm, one of the crankshaft journal axes (journal axis No. 4, counting from the camshaft sprocket side) is shifted from the others downwards by 0.03 mm

Journal No.	Angle [° CA]																							
	0	15	30	45	60	75	90	105	120	135	150	165	180	195	210	225	240	255	270	285	300	315	330	345	360
1	1978	1929	1811	1629	1384	1115	807	489	180	-98	-321	-469	-529	-492	-360	-143	141	466	807	1137	1433	1675	1850	1952	1978
2	-2570	-2422	-2061	-1510	-805	13	898	1796	2651	3407	4009	4407	4568	4471	4119	3534	2760	1856	893	-56	-921	-1643	-2175	-2488	-2570
3	7773	7454	6667	5481	3990	2301	527	-1223	-2844	-4243	-5336	-6054	-6346	-6181	-5556	-4496	-3061	-1344	536	2440	4223	5747	6896	7586	7773
4	-5712	-5324	-4373	-2926	-1070	1089	3428	5809	8082	10090	11700	12760	13190	12930	11990	10430	8367	5967	3415	905	-1579	-3279	-4677	-5499	-5712
5	-716	-881	-1250	-1857	-2757	-3989	-5549	-7370	-9314	-11190	-12770	-13840	-14270	-13970	-12980	-11430	-9517	-7479	-5531	-3845	-2522	-1591	-1021	-750	-716
6	10360	10300	10070	9779	9589	9656	10090	10900	12010	13240	14380	15190	15510	15270	14530	13410	12150	10980	10080	9555	9423	9592	9909	10210	10360
7	-6861	-6821	-6581	-6218	-5847	-5594	-5555	-5773	-6221	-6808	-7401	-7862	-8078	-7996	-7634	-7077	-6454	-5907	-5554	-5457	-5611	-5946	-6346	-6686	-6861
8	3585	3657	3682	3656	3589	3504	3428	3387	3399	3466	3573	3696	3803	3868	3872	3811	3698	3560	3428	3331	3290	3311	3383	3484	3585
9	864	789	698	613	558	547	582	655	744	826	879	888	850	776	686	603	551	543	582	658	751	836	891	901	864
10	587	603	621	636	644	642	632	616	598	583	575	577	587	604	622	637	644	643	632	615	597	582	575	576	587

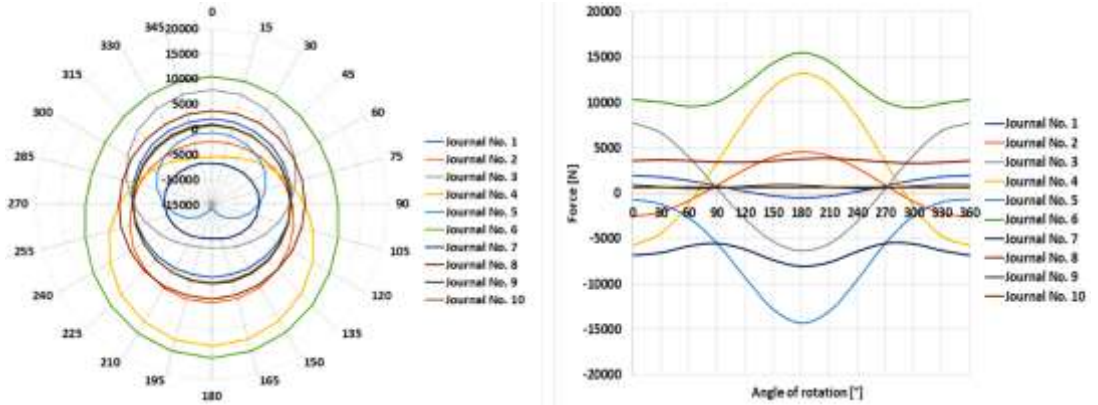

Fig. 11 Polar and Cartesian plots of vertical reaction forces where one of the main bearing socket axes (socket axis No. 6, counting from the camshaft side) is moved upwards by 0.03 mm from the others, one of the crankshaft journal axes (journal axis No. 4, counting from the camshaft side) is moved downwards by 0.03 mm from the others

Table 7 and diagrams in Fig. 12 show the values of horizontal reaction forces for the variant formulated as case no. 3.

Table 7 Distribution of horizontal reaction forces where one of the main bearing socket axes (socket axis No. 6, counting from the camshaft sprocket side) is shifted upwards from the others by 0.03 mm, one of the crankshaft journal axes (journal axis No. 4, counting from the camshaft sprocket side) is shifted from the others downwards by 0.03 mm

	Angle [° CA]																							
Journal No.	0	15	30	45	60	75	90	105	120	135	150	165	180	195	210	225	240	255	270	285	300	315	330	345	360
1	0	-301	-580	-822	-1016	-1148	-1208	-1189	-1087	-905	-651	-342	0	348	674	950	1155	1273	1298	1232	1083	867	602	307	0
2	2	891	1709	2409	2950	3301	3439	3352	3037	2509	1795	939	-2	-960	-1863	-2641	-3234	-3594	-3698	-3542	-3142	-2535	-1770	-905	2
3	-4	-1859	-3547	-4956	-6000	-6623	-6800	-6530	-5838	-4768	-3382	-1760	5	1803	3520	5034	6232	7017	7319	7106	6385	5210	3670	1886	-4
4	2	2346	4504	6353	7788	8726	9102	8880	8055	6659	4765	2491	-11	-2558	-4957	-7019	-8584	-9532	-9796	-9371	-8305	-6695	-4672	-2387	2
5	-1	-1249	-2479	-3687	-4829	-5815	-6514	-6786	-6510	-5625	-4153	-2207	18	2276	4312	5908	6916	7280	7037	6299	5216	3944	2607	1282	-1
6	1	-57	8	305	860	1605	2392	3028	3324	3149	2469	1358	-10	-1402	-2578	-3346	-3608	-3375	-2760	-1946	-1132	-486	-97	35	1
7	-1	338	591	662	504	143	-338	-814	-1153	-1252	-1066	-618	0	655	1201	1523	1559	1319	879	361	-100	-393	-459	-304	-1
8	2	-60	-145	-227	-278	-282	-234	-148	-47	40	85	79	2	-116	-255	-382	-468	-493	-453	-360	-237	-115	-24	17	2
9	-1	-57	-68	-32	41	132	215	269	279	243	170	81	-1	-53	-61	-22	53	145	229	282	291	253	177	84	-1
10	0	8	6	-4	-21	-39	-53	-61	-60	-49	-33	-15	0	8	6	-5	-21	-39	-54	-62	-60	-50	-33	-15	0

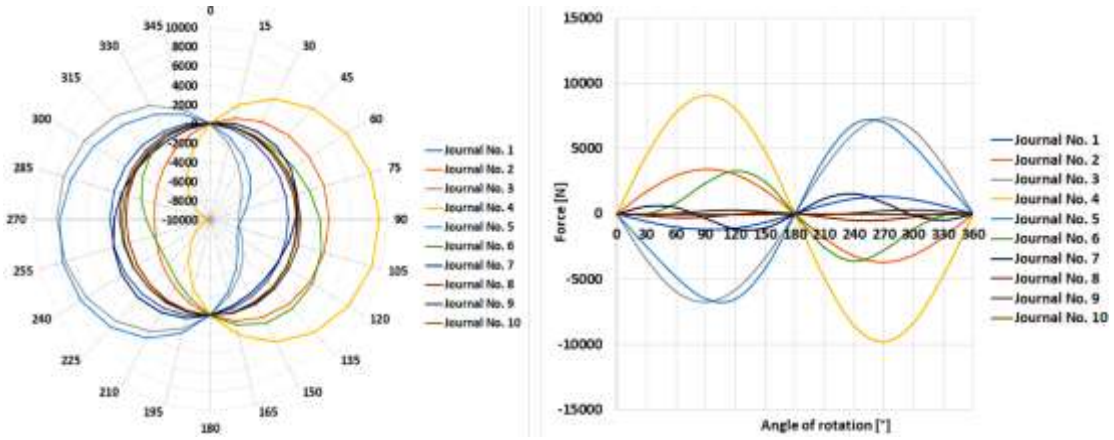

Fig. 12 Polar and Cartesian plots of the horizontal reaction force where one of the main bearing socket axes (socket axis No. 6, counting from the camshaft side) is shifted upwards from the others by 0.03 mm, one of the crankshaft journal axes (journal axis No. 4, counting from the camshaft side) is shifted from the others downwards by 0.03 mm

Given the specific difference of this case from the previously presented ones, the distribution of reduced stresses over the shaft length is shown at two opposite angular shaft positions.
The angular position was initially taken equal to 0° (Fig. 13a) and the angular position after rotation of the shaft by 180° (Fig. 13b).

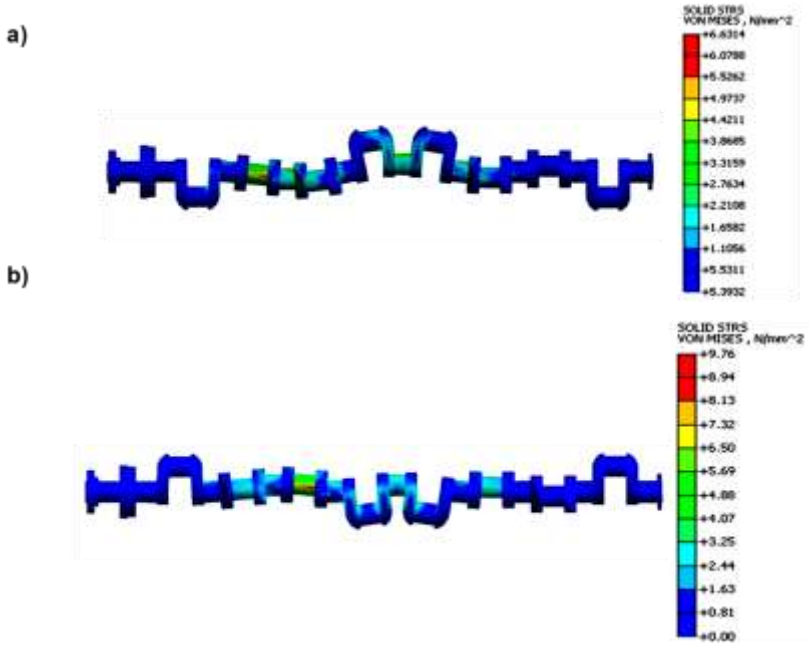

Fig. 13 Reduced stress distribution along the shaft length when one of the main bearing socket axes (socket axis No. 6, counting from the camshaft sprocket side) is moved upwards from the others by 0.03 mm, one of the main journal axes of the crankshaft (journal axis No. 4, counting from the camshaft sprocket side), is offset from the others downwards by 0.03 mm: a) angular position of the shaft is equivalent to 0°, b) the shaft is rotated 180° from the initial angular position

Table 8 and diagrams in Figure 14 (Polar and Cartesian coordinate system) show in order to illustrate the differences between the reaction forces occurring in the case of a bearing system with geometrical deviations and a bearing system with no geometrical deviations, the vertical reaction forces for a crankshaft bearing system without geometrical deviations.

Table 8 Distribution of vertical reaction forces where the shaft bearing system is not affected by geometrical deviations

	Angle [° CA]																								
Journal No.	0	15	30	45	60	75	90	105	120	135	150	165	180	195	210	225	240	255	270	285	300	315	330	345	360
1	731	726	736	758	786	813	831	836	825	803	775	749	731	726	736	758	786	813	831	836	825	803	775	749	731
2	981	999	984	939	877	815	768	750	765	810	871	934	981	999	984	939	877	815	768	750	765	810	871	934	981
3	887	839	836	879	958	1050	1131	1180	1183	1139	1061	969	887	839	836	879	958	1050	1131	1180	1183	1139	1061	969	887
4	1160	1231	1246	1203	1112	998	892	821	806	850	940	1054	1160	1231	1246	1203	1112	998	892	821	806	850	940	1054	1160
5	853	803	803	853	940	1039	1125	1175	1174	1124	1038	939	853	803	803	853	940	1039	1125	1175	1174	1124	1038	939	853
6	1081	1111	1096	1041	961	877	812	783	798	853	933	1016	1081	1111	1096	1041	961	877	812	783	798	853	933	1016	1081
7	856	806	805	854	940	1039	1125	1175	1176	1126	1041	942	856	806	805	854	940	1039	1125	1175	1176	1126	1041	942	856
8	1133	1203	1221	1183	1099	991	888	818	799	838	922	1030	1133	1203	1221	1183	1099	991	888	818	799	838	922	1030	1133
9	1023	977	964	986	1037	1105	1170	1216	1230	1208	1156	1088	1023	977	964	986	1037	1105	1170	1216	1230	1208	1156	1088	1023
10	579	590	593	587	574	557	541	531	528	533	546	563	579	590	593	587	574	557	541	531	528	533	546	563	579

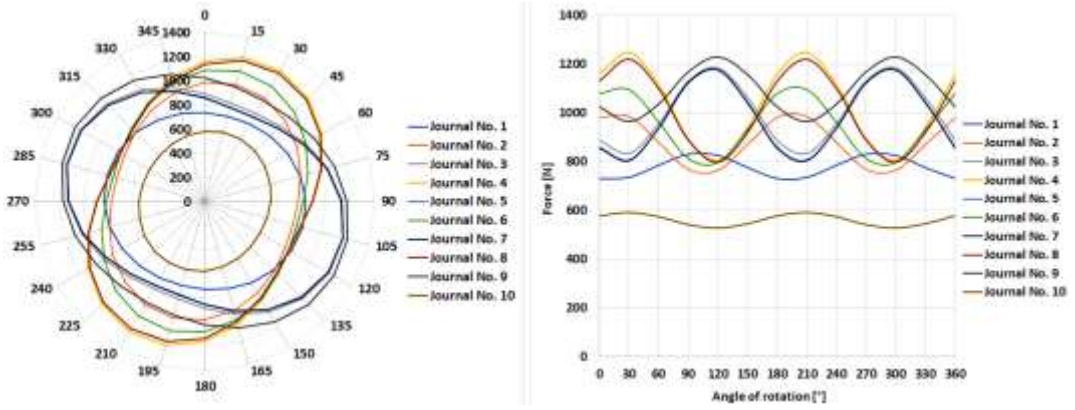

Fig. 14 Polar and Cartesian plots of vertical reaction forces for a shaft bearing arrangement not affected by geometrical deviations

The values of reaction forces are shown in Table 9 and in the diagrams in Fig. 15.

Table 9 Distribution of horizontal reaction forces where the shaft bearing system is not affected by geometrical deviations

Journal No.	Angle [° CA]																							
	0	15	30	45	60	75	90	105	120	135	150	165	180	195	210	225	240	255	270	285	300	315	330	345	360
1	-0,069	28	55	73	77	67	45	17	-10	-28	-32	-22	-0,069	28	55	73	77	67	45	17	-10	-28	-32	-22	-0,069
2	0,090	-62	-124	-171	-189	-174	-130	-68	-5	42	60	45	0,090	-62	-124	-171	-189	-174	-130	-68	-5	42	60	45	0,090
3	-0,099	78	171	252	301	304	260	181	89	8	-41	-44	-0,099	78	171	252	301	304	260	181	89	8	-41	-44	-0,099
4	0,158	-91	-205	-311	-381	-397	-353	-262	-148	-42	28	44	0,158	-91	-205	-311	-381	-397	-353	-262	-148	-42	28	44	0,158
5	0,013	86	186	272	321	321	271	185	85	-1	-50	-50	0,013	86	186	272	321	321	271	185	85	-1	-50	-50	0,013
6	-0,176	-80	-164	-229	-258	-243	-189	-109	-25	40	69	55	-0,176	-80	-164	-229	-258	-243	-189	-109	-25	40	69	55	-0,176
7	-0,171	85	185	271	321	321	272	186	87	1	-49	-49	-0,171	85	185	271	321	321	272	186	87	1	-49	-49	-0,171
8	0,475	-84	-192	-295	-365	-384	-345	-261	-153	-50	20	39	0,475	-84	-192	-295	-365	-384	-345	-261	-153	-50	20	39	0,475
9	-0,180	52	119	185	230	244	222	170	103	37	-9	-22	-0,180	52	119	185	230	244	222	170	103	37	-9	-22	-0,180
10	-0,040	-13	-30	-46	-56	-59	-54	-41	-24	-8	3	6	-0,040	-13	-30	-46	-56	-59	-54	-41	-24	-8	3	6	-0,040

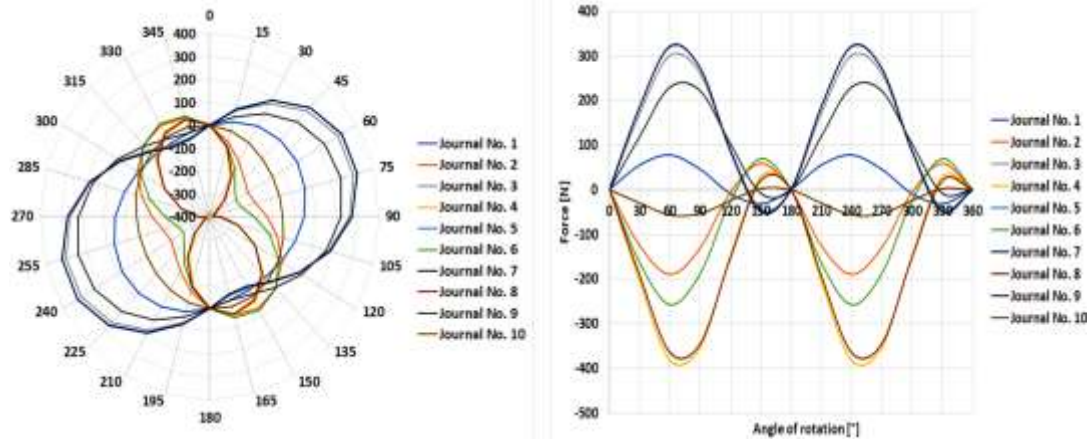

Fig. 15 Polar and Cartesian distribution diagrams of horizontal reaction forces or a shaft bearing system not affected by geometrical deviations

EVALUATION OF RESEARCH RESULTS AND CONCLUSION

The research results presented in this publication have validated the purpose of their implementation. This includes the previously suggested significant influence of geometrical deviations of the crankshaft bearing system on the values of reaction forces in main bearings and strains in crankshafts. Values of vertical and horizontal reaction forces in bearings fluctuate as demonstrated

within large ranges (which should be emphasized) due to the change of angular position of the shaft. This results in exceeding the permissible loads on the main bearings resulting in accelerated wear during motor operation. The multidirectional variability of bearing loads results in a particularly dangerous periodic loss of load bearing capacity.

It is, therefore, necessary to carry out not only measurements of shape deviations but also deviations in the position of the axles in relation to both the bearing socket hole set and the crankshaft's main journals set at the manufacturing or engine repair stage (Calculation of crankshafts for marine diesel engines, 2012; Shape and position tolerances of crankshafts – Engine technology specification MAN, 2010). Such possibilities are created by the developed measuring system with a controlled method for the implementation of variable reaction forces of the supports. The values of these forces, previously calculated using the MES (Nozdrzykowski and Chybowski, 2019; Nozdrzykowski, Chybowski and Dorobczyński, 2020) strength calculation programs, guarantee the elimination of shaft deflections and elastic deformations. Based on this solution, measurements can be carried out under conditions equivalent to those of a non-referenced measurement when the crankshaft is fixed in the counterpoints. One of the important advantages of the control unit is its stable dynamic performance characteristics. Consequently, the influence of the support conditions on the measurement of geometric values is negligible. This system allows for comprehensive measurements of geometric deviations of large crankshafts, realized in industrial conditions, as well as in repair shipyards and workshops engaged in ship engine repairs.

REFERENCES

Łukomski, Z. (1972). Technologia spalinowa silników kolejowych i okrętowych [Exhaust gas technology of railway and marine engines]; WKiŁ: Warszawa.

Kozłowiecki, H. (1974). Łożyska tłokowych silników spalinowych. Wydawnictwo Komunikacji i Łączności, Warszawa.

Basiński, H., Szyndler, S. (1984). Cienkościenne Łożyska Ślizgowe – Informator dla konstruktorów Nr 1. Wytwórnia Łożysk Ślizgowych Bimet, Gdańsk-Oliwa.

Barwell, F.T. (1984). Łożyskowanie. Wydawnictwo Naukowo-Techniczne, Warszawa.

Nozdrzykowski, K. (2013). Metodyka pomiarów geometrycznych odchyłek powierzchni walcowych wielkogabarytowych elementów maszyn na przykładzie wałów korbowych silników okrętowych. Wydawnictwo Naukowe Akademii Morskiej w Szczecinie, Szczecin, Poland.

Nozdrzykowski, K. (2017). Adjustment and analysis of forces in a flexible crankshaft support system. Journal of Machine Construction and Maintance, Problemy Eksploatacji, Nr 4(107), pp. 63-70.

Nozdrzykowski, K. (2015). Prevention of Elastic Strains in Flexible Large Size Machine Parts with the Use of Elastic Support. Machine Dynamics Research, Nr 39(2), pp. 11-122.

Nozdrzykowski, K. (2011a). System do pomiarów odchyłek geometrycznych zespołu czopów głównych wału korbowego. Pomiary Automatyka Kontrola, 57(12), pp. 1592-1594.

Nozdrzykowski, K. (2011b). Sposób i urządzenie do pomiaru odchyłek kształtu i położenia osi czopów wału korbowego. Patent pending, application P.218653, Polish Patent Office.

Calculation of crankshafts for marine diesel engines. Polish Register of Shipping. Publication 8/P, Gdańsk, Poland, 2012.

Tolerancje kształtu i położenia dla wału korbowego – specyfikacja technologiczna silników MAN B&W [Shape and position tolerances of crankshafts – Engine technology specification MAN]. H. Cegielski S.A., Poznań, Poland, 2010.

Nozdrzykowski, K., Chybowski, L. (2019). A Force-Sensor-Based Method to Eliminate Deformation of Large Crankshafts during Measurements of Their Geometric Condition. Sensors, 19(16), 3507;doi:10.3390/s19163507.

Nozdrzykowski, K., Chybowski, L., Dorobczyński, L. (2020). Model-Based Estimation of the Reaction Forces in an Elastic System Supporting Large-Size Crankshafts During Measurements of their Geometric Quantities, Measurement (2020), doi: https://doi.org/10.1016/j.measurement.107543.

Abstract: This article presents the results of a simulation, testing the variation of main bearing loads and strains in crankshafts caused by geometrical deviations of the bearing system to justify the necessity and purposefulness of measurements of both the shape and axes position deviations of crankshaft journals. Measurements of these deviations at the existing level of applied measuring techniques are significantly limited. The research also accentuates the practical implementation of a measuring system equipped with the so-called flexible support system for the measured object, developed at the Maritime University of Szczecin. This system makes it possible to eliminate elastic deformations of the crankshaft due to its own weight, whereby the measurements of geometrical deformations of the crankshafts can be carried out with appropriate accuracy in conditions corresponding to the non-reference measurements when determining the object measured in counterpoints. The obtained results have fully confirmed the purposefulness of the conducted research and the validity of the theses.

Keywords: modeling, simulation testing, loads and strains, crankshafts, bearing mounting system, geometrical deviations